A ROBUST ARBITRARILY HIGH ORDER TRANSPORT METHOD OF THE CHARACTERISTIC TYPE FOR UNSTRUCTURED TETRAHEDRAL GRIDS

R. M. Ferrer
The Idaho National Laboratory
P. O. Box 1625
Idaho Falls, ID 83415-3870
rodolfo.ferrer@inl.gov

Y. Y. Azmy
Department of Nuclear Engineering
North Carolina State University
P. O. Box 7909
Raleigh, NC 27695-7909
yyazmy@ncsu.edu

ABSTRACT

We present a robust arbitrarily high order transport method of the characteristic type for unstructured tetrahedral grids. Previously encountered difficulties have been addressed through the reformulation of the method based on coordinate transformations, evaluation of the moments balance relation as a linear system of equations involving the expansion coefficients of the projected basis, and the asymptotic expansion of the integral kernels in the thin cell limit. The proper choice of basis functions for the high-order spatial expansion of the solution is discussed and its effect on problems involving scattering discussed. Numerical tests are presented to illustrate the beneficial effect of these improvements, and the improved robustness they yield.

Key Words: Deterministic Transport, Discrete-Ordinates, Unstructured Tetrahedral Grids, High-Order, Characteristic

1. INTRODUCTION

High-order spatial discretization schemes on unstructured grids for the solution of the discrete-ordinates approximation of the transport equation have been previously proposed. In particular, the Arbitrarily High-Order Transport method of the Characteristic type in three-dimensional Unstructured Grids (AHOT-C-UG) was introduced by Azmy and Barnett [1] as an extension of the two-dimensional Cartesian-based AHOT-C approach [2]. The AHOT-C-UG methodology combines the efficient iterative solution algorithm with local coupling that the discrete-ordinates approximation provides, an arbitrarily high order spatial representation of the flux and flexible geometric representation of curved surfaces through tetrahedral meshing, while at the same time avoiding the redistribution term of the streaming operator that arises in curvilinear geometries.

In this work we present a robust AHOT-C-UG formalism designed to address the inadequate performance observed earlier with high order [1]. The three key improvements involve:

- Use of affine coordinate transformation of the tetrahedral cells into a canonical unit tetrahedron: simplifies AHOT-C-UG's formulation in general and allows for a single asymptotic expansion of the characteristic relations necessary in the thin cell limit,

- Evaluation of the moments balance relation as a linear system of equations, where the unknowns consist of the expansion coefficients of the projected basis: improves the condition number of the resulting local matrix thus leading to a stable iterative scheme,

- Asymptotic expansion of the 'spatial weights' appearing in the equations for the spatial moments of the angular flux, computed through the characteristic relations: addresses the numerical imprecision effects in the thin cell limit.

Numerical tests demonstrate the effectiveness of our improved formulation in addressing the earlier method's failures [1] and demonstrates the feasibility of performing higher order transport calculations with the AHOT-C-UG formalism via a different definition of the polynomial basis function used in the spatial expansion of the angular flux.

2. GENERAL THEORY

The exact inversion of the streaming-plus-collision operator in each cell forms the basis of short characteristic methods. This exact inversion is made possible by the fact that the S_N approximation to the neutral particle transport equation possesses straight line 'characteristic curves' along each direction $\hat{\Omega}$ in which the transport operator can be written as a total differential with respect to the characteristic length. This observation was first used by Lathrop to develop the Step Characteristics (SC) method [3] in two-dimensional Cartesian geometry, which he showed to be positive but less accurate than the conventional Diamond Difference (DD) approach. The Linear Characteristic (LC) method, an extension to the SC method, was developed in two-dimensional Cartesian geometry by Larsen and Alcouffe [4] in order to improve the accuracy of Lathrop's method. The LC method is an extension of the SC method in which the edge- and cell-averaged angular fluxes are expanded into linear basis functions. Extensions of the LC method to complex geometries, such as arbitrary polygonal and polyhedral cells, have been reported by DeHart et al [5] and Grove [6]. The possibility of improving the accuracy of the computational scheme gave rise to the Arbitrarily High-Order Transport Characteristic (AHOT-C) method, in which the edge- and cell-averaged quantities are expanded into arbitrarily high-order orthogonal polynomials [2]. The extension of the AHOT-C formalism into three-dimensional unstructured grids, namely the AHOT-C-UG methodology, requires the use of coordinate transformations in order to achieve the desired robustness. The coordinate transformation adopted in this work is similar to the approach proposed by Mathews et al [7] for unstructured tetrahedral grids.

2.1. Potential Characteristic Tetrahedron (CT) Configurations

Similar to the cell splitting procedure in AHOT-C, the use of the characteristic relation in AHOT-C-UG will require the splitting of the arbitrary tetrahedron into subcell tetrahedra. The number of subcell tetrahedra and their shape for a given tetrahedral cell will depend on the angular direction under consideration. Such subcell tetrahedra will be referred to as a Characteristic

2009 International Conference on Mathematics, Computational
Methods & Reactor Physics (M&C 2009), Saratoga Springs, NY, 2009

2/15

Tetrahedron (CT). The CT configurations define the splitting or slicing of a tetrahedral cell into constituent CTs with respect to a discrete angular direction $\hat{\Omega}$. More specifically, an arbitrary tetrahedron may be split into CTs depending on the number of incoming and outgoing cell faces with respect to the particle direction of motion. The total number of potential configurations depends on the cell shape. For the particular instance of a tetrahedron, three configurations are possible: one incoming face and three outgoing faces, two incoming and two outgoing faces, and three incoming faces and one outgoing face. These three general cases are sketched in Fig. 1.

In the first case, in which there is one incoming and three outgoing faces, the characteristic relation is used to calculate the outgoing face angular flux at each of the faces by splitting the incoming face into three triangles that serve as bases of the resulting CTs. In the second case, in which there are two incoming and two outgoing faces, the incoming faces are split, and the characteristic relation is used to compute the outgoing angular flux through four CTs. Once the CT outgoing angular fluxes are computed, the two CT outgoing angular fluxes per cell face are projected into a single face. Finally, in the case of three incoming and one outgoing angular flux, the characteristic relation is used to compute the outgoing angular flux through three CTs, and the three outgoing angular fluxes are projected into a single face. Once all the cell face angular fluxes have been computed, the cell balance of all retained moments is applied over the entire tetrahedral cell and the cell-moments of the angular flux are computed.
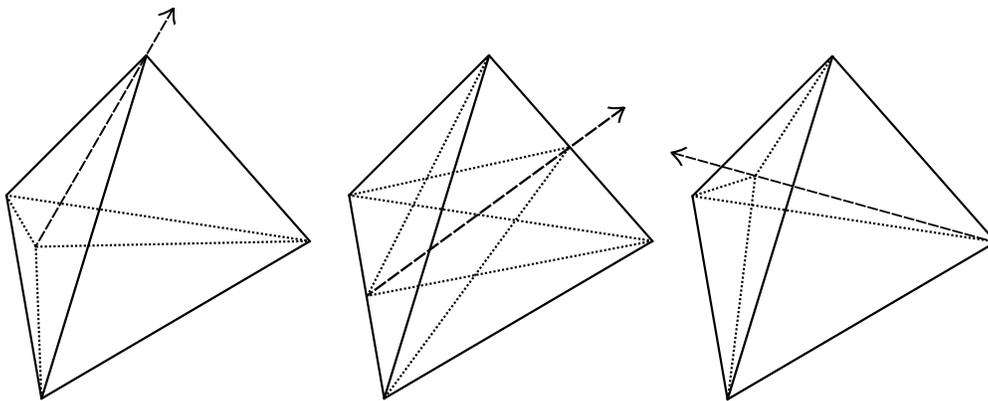

Figure 1. Potential Characteristic Tetrahedron (CT) configurations for non-planar angular direction

In addition to the CT configurations described above, there are three *degenerate* cases, in which the orientation of the arbitrary tetrahedron may cause one of its faces to coincide with the angular direction $\hat{\Omega}$. In general, there are three degenerate cases: two incoming faces and one outgoing face, one incoming face and two outgoing faces, and one incoming and one outgoing face. These are shown schematically in Fig. 2. In the first case, two incoming face angular fluxes may split the tetrahedron into two CTs due to the angular direction being parallel to one of the cell faces. Once these two CTs are used to compute the outgoing CT angular flux via the characteristic equation, the two outgoing angular fluxes are projected into a single outgoing cell face. In the second case, one incoming face angular flux may split the tetrahedron into two CTs, where the incoming face angular flux is split and the two cell face outgoing angular fluxes can be readily obtained from the two CTs. Finally, the third degenerate case is the trivial case in which the cell is

2009 International Conference on Mathematics, Computational
Methods & Reactor Physics (M&C 2009), Saratoga Springs, NY, 2009

3/15

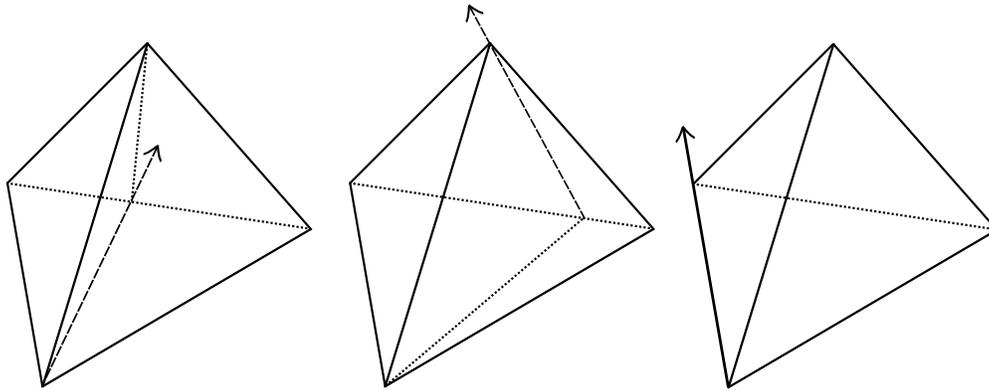a CT, thus there is only a single incoming and outgoing cell face.

Figure 2. Degenerate Characteristic Tetrahedron (CT) configurations for planar coincidental angular direction

An algorithm that determines the CT configurations with respect to the cell orientation can be devised by simply testing the number of incoming and outgoing cell faces. Since the unstructured nature of the geometric description makes it impossible to determine *a priori* the sweeping order, each cell is examined throughout the sweep to determine how it's equations can be solved for the outgoing face angular fluxes. This determination and the necessary transformations are performed on-the-fly.

2.2. Affine Coordinate Transformation Among Global, Cell, and CT Coordinate Systems

Unlike the case of AHOT-C, in which the computational cell edges coincide with a global Cartesian coordinate systems, the AHOT-C-UG formalism requires the transformation of an arbitrary tetrahedral cell into a unit tetrahedral cell. This transformation simplifies the derivation of the final set of discrete-variable equations and allows for a single asymptotic expansion of the 'characteristic kernel', i.e. integral form of the characteristic relation along the streaming direction. First, consider an arbitrary tetrahedron with respect to a global Cartesian coordinate system as illustrated in Fig. 3.

The global coordinate system is assumed to be an orthogonal Cartesian system where a point located at the coordinates (x_1^j, x_2^j, x_3^j) is specified by the j-th position vector $\vec{r}^j$,

$$\vec{r}^j = x_i^j \, \hat{e}_i \tag{1}$$

where $\hat{e}_i$ are unit vectors that define the global Cartesian coordinate system. Note that Einstein summation convention has been introduced, in which repeated latin indices are summed over. Let $\{\vec{r}^0, \vec{r}^1, \vec{r}^2, \vec{r}^3\}$ be a set of vectors that specify the position of the four vertices that define a tetrahedral *cell* with respect to the global Cartesian coordinate system. The first task is to define an affine transformation that maps an arbitrary tetrahedron into a unit tetrahedron. This procedure will simplify the computation of face- and volume-moments over the computational cell. The vector basis for the local cell-coordinate system is defined with respect to the cell vertices
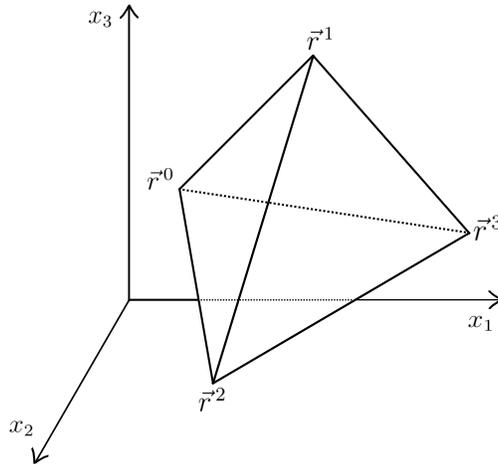
2009 International Conference on Mathematics, Computational
Methods & Reactor Physics (M&C 2009), Saratoga Springs, NY, 2009

4/15

Figure 3. Arbitrary tetrahedron in global Cartesian coordinates

position vectors in the following manner,

$$\vec{U}_j = \vec{r}^{\,j} - \vec{r}^{\,j-1} \qquad j = 1, 2, 3 \tag{2}$$

Thus, any arbitrary tetrahedral cell may be mapped into a local coordinate system as prescribed by Eq. (2). An illustration of the local cell coordinate system is shown in Fig. 4. Note that the transformation automatically normalizes the arbitrary tetrahedron into a 'canonical' form that has unit side lengths in the cell coordinate system.
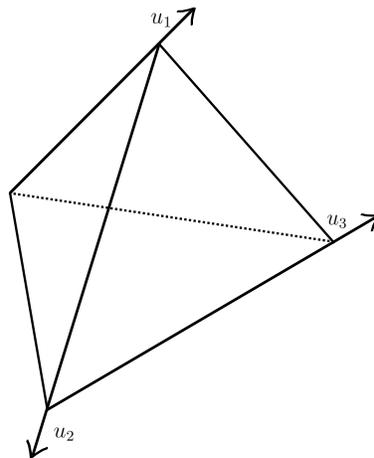

Figure 4. Normalized tetrahedron in local coordinates

Now that the global and cell coordinate systems have been defined, it is possible to express any point $\vec{r}$ *inside* a certain arbitrary tetrahedron to vector $\vec{u}$ *inside* the transformed unit tetrahedron and vice versa through the relation

$$\vec{r} = \vec{r}^{\,0} + \vec{U}_1 u_1 + \vec{U}_2 u_2 + \vec{U}_3 u_3 \tag{3}$$

2009 International Conference on Mathematics, Computational
Methods & Reactor Physics (M&C 2009), Saratoga Springs, NY, 2009

5/15

where the basis vectors on the right hand side of Eq. (3) are defined by Eq. (2). Thus, Eq. (3) transforms a vector $\vec{u}$ in the cell coordinate system, into the vector $\vec{r}$ in the global coordinate system. This transformation can be written as

$$\vec{r} = \vec{r}^{0} + \boldsymbol{J}\vec{u} \tag{4}$$

where $\boldsymbol{J}$ is known as the Jacobian matrix

$$\boldsymbol{J} = \begin{bmatrix} x_1^1 - x_1^0 & x_1^2 - x_1^1 & x_1^3 - x_1^2 \\ x_2^1 - x_2^0 & x_2^2 - x_2^1 & x_2^3 - x_2^2 \\ x_3^1 - x_3^0 & x_3^2 - x_3^1 & x_3^3 - x_3^2 \end{bmatrix} \tag{5}$$

The determinant of the Jacobian matrix, denoted by $\|\boldsymbol{J}\|$, has the important property that allows for the transformation of integral quantities over a certain domain in the global system into the equivalent quantity projected into the cell coordinate system. Identical transformation relations may be derived for the *subcell* tetrahedra inside the tetrahedral cell.

Analogous to the cell and CT transformations described above, it will be necessary to perform similar transformations on the cell faces. Unlike the case of AHOT-C in Cartesian geometry, the cell faces are not normal to the axes of the global coordinate system and thus need special treatment. Similar transformation and face Jacobian matrices can be defined for the cell and CT face coordinate systems. In summary, all transformations of the cells and CTs into local face- and volume-coordinate systems are performed through the use of Jacobian matrices and their determinants. Now that the geometry preliminaries have been covered, the AHOT-C-UG formalism will be presented.

2.3. The Arbitrarily High Order Transport Method of Characteristic Type (AHOT-C)

The starting point for deriving the AHOT-C-UG method is the moments balance equation, in which the transport equation is multiplied by a 'test' or basis function and integrated over the spatial domain. Let $B_{\vec{i}}(\vec{r})$ denote a polynomial basis function of order $\vec{i} = \{i_j, j = 1, 2, 3\}$, where the i_j satisfies $(0 \leq i_1 + i_2 + i_3 \leq \Lambda)$ if a 'complete' basis is used or $(0 \leq i_j \leq \Lambda, j = 1, 2, 3)$ if a 'double' Pascal tetrahedron is used, in which case the mixed moments are always retained by the expansion. In both cases, Λ denotes the highest order of the polynomial basis, and thus determines the spatial expansion order of the method. The steady-state, mono-energetic, discrete-ordinates approximation of the transport equation is

$$\hat{\Omega} \cdot \vec{\nabla}\psi(\vec{r}) + \sigma_T(\vec{r})\psi(\vec{r}) = S(\vec{r}) \tag{6}$$

where the total and scattering macroscopic cross-sections are denoted as σ_T and σ_{sc}, respectively, and $S(\vec{r})$ is the distributed source. By multiplying Eq. (6) by the basis function and integrating over the cell domain, the $\vec{i}$-th moment balance equation is obtained

$$\frac{1}{V} \int_V dV \, B_{\vec{i}}(\vec{r})\{\hat{\Omega} \cdot \vec{\nabla}\psi(\vec{r}) + \sigma_T\psi(\vec{r}) = S(\vec{r})\} \tag{7}$$

Applying Green's Theorem to the streaming term of Eq. (7) yields

$$\frac{1}{V} \int_V dV \, B_{\vec{i}}(\vec{r})(\hat{\Omega} \cdot \vec{\nabla}\psi(\vec{r})) = \frac{1}{V} \int_A dA(\hat{n} \cdot \hat{\Omega}) B_{\vec{i}}(\vec{r})\psi(\vec{r})$$
$$- \frac{1}{V} \int_V dV \, \psi(\vec{r})(\hat{\Omega} \cdot \vec{\nabla}B_{\vec{i}}(\vec{r})) \tag{8}$$

2009 International Conference on Mathematics, Computational
Methods & Reactor Physics (M&C 2009), Saratoga Springs, NY, 2009

6/15

At this point it is necessary to consider the effects of transforming between the global and local cell coordinate systems. Specifically, if Eq. (8) is to be evaluated locally in the cell coordinate system, then it is necessary to re-write the streaming operator $\hat{\Omega} \cdot \vec{\nabla} B_{\vec{i}}(\vec{r})$ on the right hand side as

$$\hat{\Omega} \cdot \vec{\nabla} B_{\vec{i}}(\vec{r}) = \hat{\Omega} \cdot \left(\sum_{k=1}^{3} \frac{\partial}{\partial x_k} B_{\vec{i}}(\vec{r}) \hat{e}_k \right)$$
$$= \hat{\Omega} \cdot \left(\sum_{k=1}^{3} \frac{\partial u_j}{\partial x_k} \frac{B_{\vec{i}}(\vec{u})}{\partial u_j} \hat{e}_k \right) \quad (9)$$

where the repeated subscript j indicates summation. In order to further simplify the above relation, let $\hat{\Omega} = (\mu_1, \mu_2, \mu_3)$. Noting that $\frac{\partial u_j}{\partial x_k}$ denotes the *inverse* of the Jacobian matrix defined in Eq. (5), Eq. (9) becomes

$$\hat{\Omega} \cdot \vec{\nabla} B_{\vec{i}}(\vec{r}) = \mu_k J_{jk}^{-1} \frac{B_{\vec{i}}(\vec{u})}{\partial u_j} \quad (10)$$

The specific choice of basis functions for AHOT-C-UG in the cell coordinate system will be the monomial basis $B_{\vec{i}}(\vec{u}) = u_1^{i_1} u_2^{i_2} u_3^{i_3}$ and in the cell *face* coordinate system $B_{\vec{i}}(\vec{u}^F) = (u_1^F)^{i_1}(u_2^F)^{i_2}$. The cell face or *area* moment, and cell *volume* moments, are defined as

$$\psi_{\vec{i}}^F \equiv \frac{1}{A^F} \int_{A^F} dA^F B_{\vec{i}}(\vec{r}) \psi(\vec{r}) \quad (11)$$

$$g_{\vec{i}} \equiv \frac{1}{V} \int_V dV B_{\vec{i}}(\vec{r}) g(\vec{r}) \quad (12)$$

respectively, where $g(\vec{r}) = \psi(\vec{r}), \phi(\vec{r})$, or $S(\vec{r})$. Finally, by substituting Eq. (10), and definitions (11) and (12) into Eq. (8), the resulting expression for the transformed streaming term of the balance equation is obtained

$$\frac{1}{V} \int_V dV B_{\vec{i}}(\vec{r})(\hat{\Omega} \cdot \vec{\nabla} \psi(\vec{r})) = \frac{1}{V} \sum_{F=0}^{3} (\hat{n}^F \cdot \hat{\Omega}) A^F \psi_{\vec{i}}^F - \mu_k J_{jk}^{-1} i_j \psi_{\vec{i}-\hat{j}} \quad (13)$$

where $\psi_{\vec{i}-\hat{j}}$ denotes a lower-order spatial moment of the angular flux, arising from differentiating the monomial basis function. Finally, the $\vec{i}$-th moment balance equation is obtained

$$\frac{1}{V} \sum_{F=0}^{3} (\hat{n}^F \cdot \hat{\Omega}) A^F \psi_{\vec{i}}^F - \mu_k J_{jk}^{-1} i_j \psi_{\vec{i}-\hat{j}} + \sigma_T \psi_{\vec{i}} = S_{\vec{i}} \quad (14)$$

Equation (14) represents the $\vec{i}$-th spatial moment balance for an arbitrary tetrahedral cell in the global coordinate system *evaluated* in the local cell coordinate system. Since the zeroth-moment is equivalent to the average angular flux over cell, and thus remains invariant under transformation, the cell-average angular flux is identical in both the global and local coordinate systems. This property can be verified by noting that the lower-order moment term on the left hand side of Eq. (14) that contains elements of the Jacobian matrix is not evaluated for the zeroth-moment. Furthermore, all non-zero moments represent spatial moments in the local cell coordinate system, thus readily allowing for the evaluation of the local distributed source in the presence of scattering and fission.

2009 International Conference on Mathematics, Computational Methods & Reactor Physics (M&C 2009), Saratoga Springs, NY, 2009

7/15

A similar form of Eq. (14), the moment balance equation, had been previously derived by Azmy and Barnett [1]. A recursive scheme was devised by the authors such that higher-order moments are computed from lower-order moments. This recursive scheme, which can be alternatively viewed as a lower triangular matrix form which is solved for the moments via forward substitution, was found to produced inaccurate higher-order moments of the angular flux for *optically thin cells*. These inaccuracies in the high-order moments are due to the ill-conditioning of the lower triangular matrix, which is caused by the fact that the 'pivot' elements in the matrix involve a σ_T term. Thus, the solution of the matrix via forward substitution causes the accumulation of roundoff error for very small σ_T as the higher-order moments are solved for in terms of lower-order moments. In fact, Eq. (14) was implemented in the work presented here and similar numerical issues were observed. In order to circumvent the problem, Eq. (14) was re-cast in terms of *expansion* coefficients. This procedure stabilized the numerical algorithm by casting the problem into a non-triangular matrix form and then dividing the final system of equations by σ_T, which improved the conditioning of the system even as the cell becomes optically thin. Unlike the case of orthogonal functions in structured geometries, in which orthogonal functions such as Legendre polynomials are used in rectangular cells, the use of monomials requires the solution of a linear system of equations in order to obtain the expansion coefficients. For instance, if the function $g(\vec{r})$, in definition (12), is expanded locally into the set of 'trial' basis functions such that $g(\vec{u}) = \sum_{\vec{i}'=0}^{\Lambda} G_{\vec{i}'} B_{\vec{i}'}(\vec{u})$, then the expansion coefficients and moments are related by

$$\vec{g}_{\vec{i}} = \boldsymbol{M} \vec{G}_{\vec{i}'} \tag{15}$$

where matrix $\boldsymbol{M}$ is the tensor product of the monomial basis and is also known as the mass matrix in finite element methods nomenclature. Similarly, the Jacobian term in Eq. (14) can be related to the expansion coefficients via

$$\mu_k J_{jk}^{-1} i_j \vec{\psi}_{\vec{i}-\hat{j}} = \boldsymbol{D} \vec{\Psi}_{\vec{i}'} \tag{16}$$

where matrix $\boldsymbol{D}$ is known as the stiffness matrix in finite element methods nomenclature. It is now possible to recast Eq. (14) by substituting relations (15), in particular $\vec{\psi}_{\vec{i}} = \boldsymbol{M} \vec{\Psi}_{\vec{i}'}$, and (16) into the balance equation, thus producing the balance equation in terms of the angular flux expansion coefficients

$$\left(-\boldsymbol{D} + \sigma_T \boldsymbol{M} \right) \vec{\Psi}_{\vec{i}'} = \vec{S}_{\vec{i}} - \frac{1}{V} \sum_{F=0}^{3} (\hat{n}^F \cdot \hat{\Omega}) A^F \vec{\psi}_{\vec{i}}^F \tag{17}$$

The solution to Eq. (17) as a system of linear equations via numerical inversion can still become problematic as the cell becomes optically thin due to the loss of precision in the computation of the angular flux face-moments via the characteristic relation. In order to resolve this issue, Eq. (17) is divided by σ_T, yielding the expression

$$\left(-\frac{1}{\sigma_T} \boldsymbol{D} + \boldsymbol{M} \right) \vec{\Psi}_{\vec{i}'} = \frac{\vec{S}_{\vec{i}}}{\sigma_T} - \frac{1}{V} \sum_{F=0}^{3} (\hat{n}^F \cdot \hat{\Omega}) A^F \frac{\vec{\psi}_{\vec{i}}^F}{\sigma_T} \tag{18}$$

where elements of matrices $\boldsymbol{D}$ and $\boldsymbol{M}$ are known exactly, the source is assumed to be an external source or to have come from a previous iteration, and the face angular fluxes $\vec{\psi}_{\vec{i}}^F / \sigma_T$ are assumed to be either known from either an upstream cell or computed through the characteristic relation. In fact, asymptotic expressions which involve the division of face angular flux moments by σ_T will be derived shortly in order to provide an accurate representation of the right hand side of (18).

2009 International Conference on Mathematics, Computational
Methods & Reactor Physics (M&C 2009), Saratoga Springs, NY, 2009

8/15

2.3.1. Asymptotic Expansion of the Arbitrarily High-Order Characteristic Relation

The outgoing face-angular flux for a Characteristic Tetrahedron (CT), with known incoming and source spatial moments, is given by the characteristic relation. This characteristic relation comes from the exact inversion of the streaming-plus-collision operator of the transport equation. In the CT coordinate system (q_1, q_2, q_3), defined by $\vec{Q}_j = \vec{r}_{ct}^{\,j} - \vec{r}_{ct}^{\,j-1}(j = 1, 2, 3)$, the characteristic relation has the following form

$$\psi^{f,out}(\vec{q}) = \psi^{f,in}(\vec{q})e^{-\epsilon q_3} + \tau \int_0^{q_3} S^v(\vec{q})e^{-\epsilon(q_3 - q_3')}dq_3' \tag{19}$$

where $\psi^{f,in}(\vec{q})$ is the incoming CT face angular flux, $S^v(\vec{q})$ is the CT distributed source, $\epsilon \equiv \sigma_T \tau$ is the cell optical thickness, and τ is the physical thickness of each cell with respect to the angular direction under consideration and the CT configuration. The outgoing face moments in the CT *face* coordinate system (q_1^f, q_2^f), defined by $\vec{Q}_j^f = \vec{r}^{f,j} - \vec{r}^{f,j-1}(j = 1, 2)$, are computed via the relation

$$\vec{\psi}_{\vec{i}f}^{f,out} = \frac{1}{A^f} \int_{A^f} dA^f B_{\vec{i}f}^{f,out}(\vec{r})\psi^{f,out}(\vec{r}) \tag{20}$$

where $B_{\vec{i}f}(\vec{r}^f)$ is the basis function in the CT outgoing face coordinate system. By substituting (19) into (20), and dividing by σ_T, the following expression is obtained

$$\vec{\psi}_{\vec{i}f}^{f,out}/\sigma_T = \boldsymbol{F}\vec{\Psi}_{\vec{i}f'}^{f,in}/\sigma_T + \boldsymbol{V}\vec{S}_{\vec{i}'}^{v}/\sigma_T \tag{21}$$

where matrices $\boldsymbol{F}$ and $\boldsymbol{V}$ can be evaluated analytically. The explicit analytical evaluation of the elements of the matrices $\boldsymbol{F}$ and $\boldsymbol{V}$, can cause numerical loss-of-precision as cells become optically thin. A more robust evaluation can be obtained by performing an asymptotic expansion. Defining the following parameters

$$\gamma_1 \equiv i_1^{f'} + i_1^f \tag{22a}$$

$$\gamma_2 \equiv i_2^{f'} + i_2^f \tag{22b}$$

$$\gamma_3 \equiv i_3^{f'} \tag{22c}$$

and expanding the exponential function in Eq. (19) into the Taylor series expansion

$$e^{\pm \epsilon q_3} = \sum_{n=0}^{\infty} \frac{(\pm 1)^n}{n!} \epsilon^n (q_3)^n \tag{23}$$

the following asymptotic expressions for the matrix elements can be obtained

$$\boldsymbol{F} = 2 \sum_{n=0}^{\infty} \frac{(-1)^n}{n!} \frac{\epsilon^n}{(\gamma_1 + \gamma_2 + n + 2)(\gamma_2 + n + 1)} \tag{24}$$

$$\boldsymbol{V} = 2\tau \sum_{n=0}^{\infty} \sum_{m=0}^{\infty} \frac{(-1)^m \epsilon^{n+m}}{n!m!(\gamma_1 + \gamma_2 + \gamma_3 + n + m + 3)(\gamma_2 + \gamma_3 + n + m + 2)(\gamma_3 + n + 1)} \tag{25}$$

Once the CT outgoing face angular flux moments are computed through the characteristic relation, based on the CT incoming face angular flux moments and the distributed source moments, the balance relation can be solved by combining all outgoing CT face moments in accordance to the CT configurations described in previous sections.

2009 International Conference on Mathematics, Computational
Methods & Reactor Physics (M&C 2009), Saratoga Springs, NY, 2009

9/15

2.4. Pascal Pyramid versus Double Pascal Pyramid Basis Functions

An aspect that is currently under investigation is the choice of monomial basis functions in which to represent the face and volume angular fluxes. While the AHOT-C formulation in Cartesian geometry [2] used Legendre polynomials as basis functions that retain all the mixed term, the use of a monomial basis that retains mixed terms has been found numerically unstable in the AHOT-C-UG formulation. This numerical instability manifests itself in the divergence of the inner iterations, specifically in a highly scattering medium where many iterations are required to achieve convergence, thus allowing round-off errors to accumulate sufficiently and cause the iterations to fail to converge. We note that the numerical results presented in the next section correspond to the case in which the basis is considered to be complete, such that $\vec{i} = \{i_j, j = 1, 2, 3\}$ satisfies $(0 \leq i_1 + i_2 + i_3 \leq \Lambda)$

3. Numerical Results

In order to verify the formulation of AHOT-C-UG, and its implementation into the new Tetrahedral High Order Radiation (THOR) transport code written in FORTRAN 90, the test problems presented in [1] were used in this exercise. A 3 x 3 x 3 mean-free-path (mfp) cube in a medium with $\sigma_T = 1$ and four possible values of $\sigma_{sc} = 0, 0.1, 0.5$, and 0.9 was subdivided into 27 unit subcubes at each refinement level and solved with THOR. The mesh refinement studies were performed by subdividing each of the 27 unit subcubes by two in each dimension, resulting in eight new subcubes per unit subcube. Each of these subcubes are subsequently tessellated into five tetrahedrons, as shown in Fig. 5. A total of five meshes, ranging from 135 to 552,960 tetrahedral cells, were generated in order to test the convergence behavior of the AHOT-C-UG methodology.
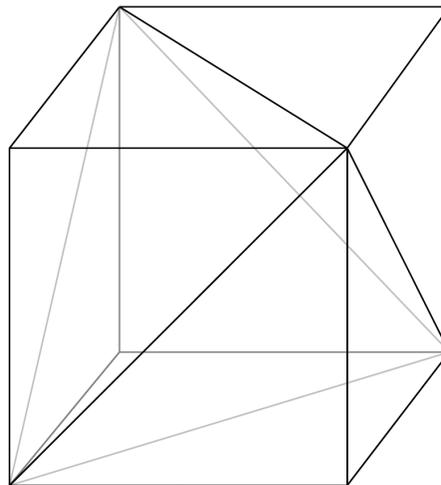

Figure 5. Subcube tessellated into five tetrahedrons

Two versions of the configuration discussed above were used to determine the solution accuracy: problems with analytical solutions and problems with numerical reference solutions. The problems with analytical solutions do not include scattering and involve two variants: a problem

2009 International Conference on Mathematics, Computational
Methods & Reactor Physics (M&C 2009), Saratoga Springs, NY, 2009

10/15

with a flat distributed source and vacuum boundary conditions, and a problem with constant incoming boundary sources on three external faces, but no distributed sources. The problems in which numerical reference solutions are computed involve three scattering ratios: $c = 0.1, 0.5, 0.9$, where c is defined as $c = \sigma_{sc}/\sigma_T$. The maximum absolute-value of the error between the approximate and reference solution (L_∞ error norm) is computed over each of the 27 subcubes for the averaged scalar flux.

3.1. Problems with Analytical Solutions: Cube with Purely Absorbing Medium

The analytical solution for the average scalar flux in each unit subcube, based on a single angular direction (one octant in an S_2 quadrature), was derived to serve as reference value. Each subcube was tessellated and THOR was used to solve for the average angular flux in each cell. The average scalar flux in each cell was computed from the angular flux via the S_2 quadrature formula, and subsequently spatially integrated over the unit subcubes. An error norm based on each subcube's exact and approximate average scalar fluxes, Φ_i and ϕ_i respectively, was defined as $\|e\|_\infty \equiv max\{|\Phi_i - \phi_i|\}$, $i = 1, ..., 27$ and computed for the flat source and boundary source problems. A total of 5 meshes and five spatial approximation orders, based on the complete basis for $\Lambda = 0, ..., 4$, were used to solve this problem. The plots of the error norms for the flat source and fixed boundary source problems are shown in Figs. 6 and 7, respectively. Evident from these plots is the decrease of the maximum error in the asymptotic regime with mesh refinement, which supports correctness of the implementation. Furthermore, the order of accuracy obtained from fitting a polynomial to the plotted points on each curve, of the maximum error is listed next to the curves and is observed to increase as the spatial expansion order is increased. It is interesting to note the "fractional" increase in this order as the polynomial spatial approximation order of the angular flux is also increased.

3.2. Problems with Numerical Solutions: Cube with Scattering

The second set of problems is designed to test the higher order spatial representation of the angular flux, via its influence on the scattering term. A reference fine-mesh TORT [8] calculation, with approximately 1 billion cells, was used in this case for the computation of the reference solution. In order to complete the calculations within a reasonable execution time, only four meshes were used in THOR for the $\Lambda = 0, ..., 3$. Similar to the first set of problems results, Figs. 8 through 10 illustrate that the maximum error decreases in the asymptotic regime with mesh refinement and the order of accuracy increases as the spatial expansion order increases, exhibiting a similar "fractional" increase in the order of accuracy.

4. CONCLUSIONS

We have presented an improved AHOT-C-UG methodology that circumvents previous difficulties by introducing coordinate transformations, asymptotic expansion of the integral kernels, and the solution of a linear system representing the cell particle balance. Numerical results are provided to support our ultimate objective of demonstrating the feasibility and accuracy of the method.
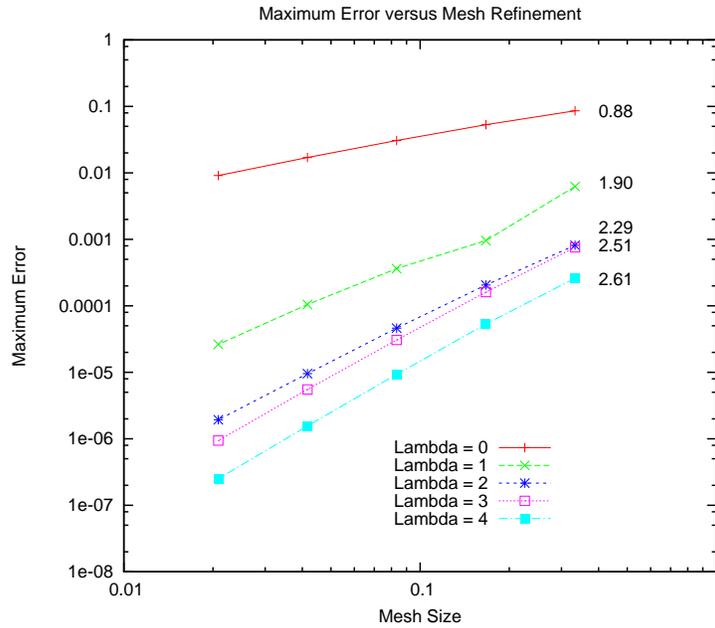
2009 International Conference on Mathematics, Computational
Methods & Reactor Physics (M&C 2009), Saratoga Springs, NY, 2009

11/15

Figure 6. Log-log plot of the L_∞ error norm of the scalar flux over the 27 subcubes and order of convergence for the flat source problem with c=0.0
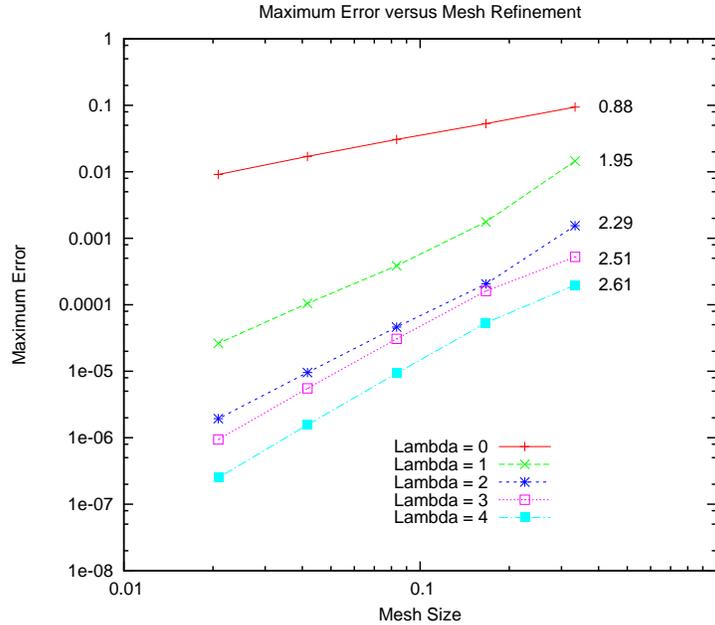

Figure 7. Log-log plot of the L_∞ error norm of the scalar flux over the 27 subcubes and order of convergence for fixed incoming boundary source problem

2009 International Conference on Mathematics, Computational
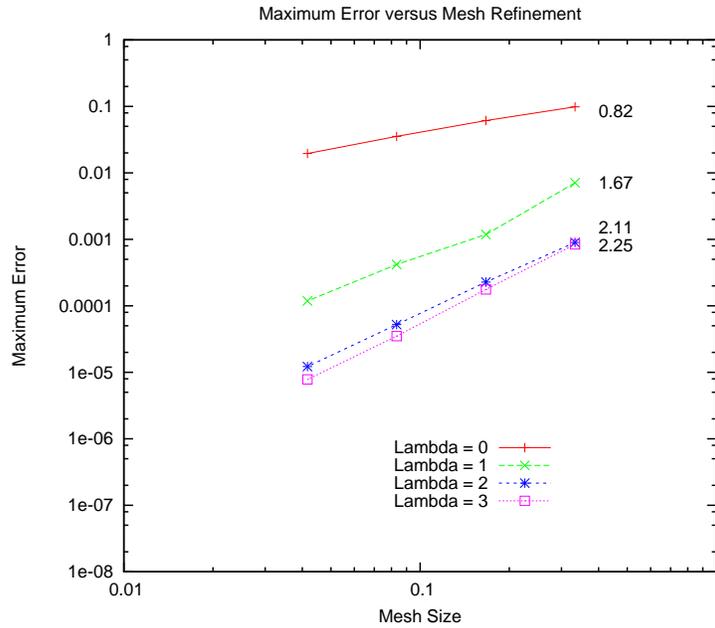Methods & Reactor Physics (M&C 2009), Saratoga Springs, NY, 2009

12/15

Figure 8. Log-log plot of the L_∞ error norm of the scalar flux over the 27 subcubes and order of convergence for flat source problem with c=0.1
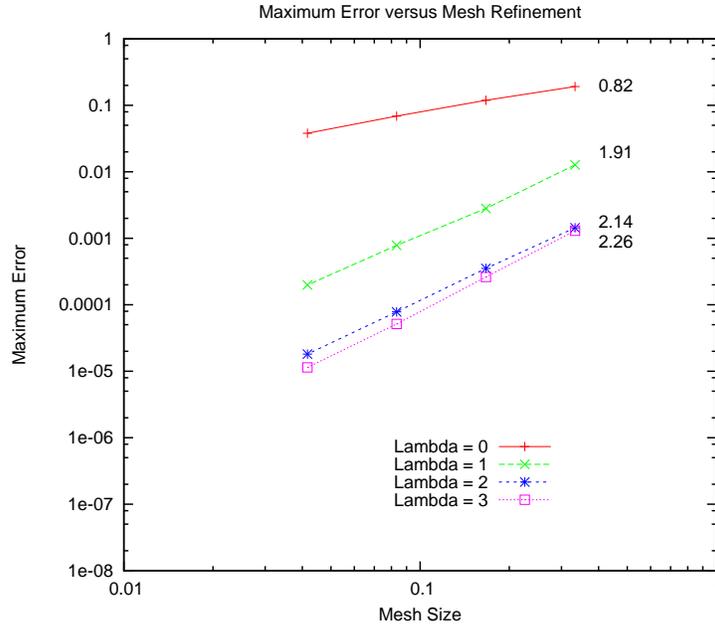

Figure 9. Log-log plot of the L_∞ error norm of the scalar flux over the 27 subcubes and order of convergence for flat source problem with c=0.5

2009 International Conference on Mathematics, Computational
Methods & Reactor Physics (M&C 2009), Saratoga Springs, NY, 2009
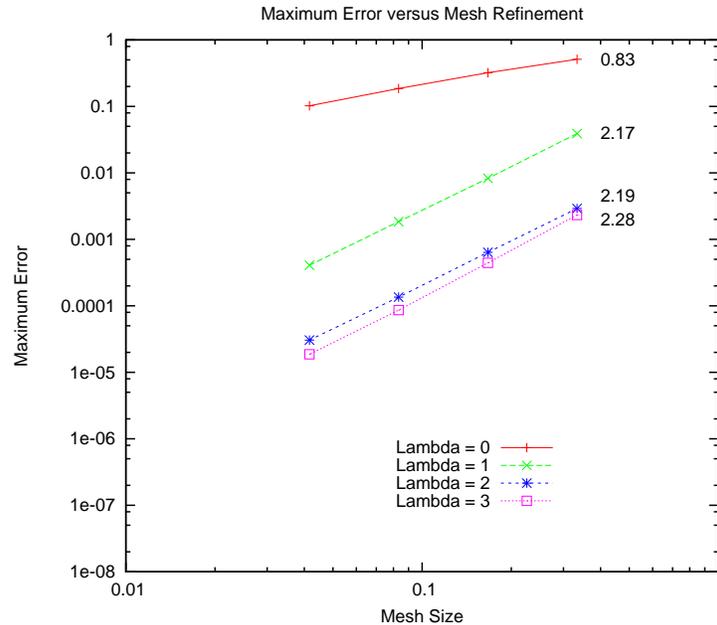
13/15

Figure 10. Log-log plot of the L_∞ error norm of the scalar flux over the 27 subcubes and order of convergence for flat source problem with c=0.9

ACKNOWLEDGEMENTS

REFERENCES

[1] Y. Y. Azmy and D. A. Barnett, "Arbitrarily High Order Transport Method of the Characteristic Type for Tetrahedral Grids," *Proceedings of ANS International Meeting on Mathematical Methods for Nuclear Applications 2001*, Salt Lake City, Utah, September 9-13, (2001).

[2] Y. Y. Azmy, "Arbitrarily High Order Characteristic Methods for Solving The Neutron Transport Equation," *Annals of Nuclear Energy*, **19**, pp. 593-606 (1992).

[3] K. D. Lathrop, "Spatial Differencing of the Transport Equation: Positivity vs. Accuracy," *Journal of Computational Physics*, **4**, pp. 475-498 (1969).

[4] E. W. Larsen and R. E. Alcouffe, "The Linear Characteristic Method for Spatially Discretizing the Discrete-Ordinates Equations in (X,Y)-Geometry," *Proceedings of Int. Topl. Mtg. Advances in Mathematical Methods for the Solution of Nuclear Engineering Problems*, Munich, Germany, Kernforschungszentrum Karlsruhe, (1981).

[5] M. D. DeHart, R. E. Pevey, and T. A. Parish, "An Extended Step Characteristic Method for Solving the Transport Equation in General Geometries," *Nuclear Science and Engineering*, **118**, pp. 79-90 (1994).

2009 International Conference on Mathematics, Computational Methods & Reactor Physics (M&C 2009), Saratoga Springs, NY, 2009

14/15

[6] R. E. Grove, "The Slice Balance Approach (SBA): A Characteristic-Based, Multiple Balance S_N Approach on Unstructured Polyhedral Meshes," *Proceedings of Joint Int. Topl. Meeting on Mathematics and Computations, Supercomputing, Reactor Physics and Nuclear and Biological Applications, M and C 2005*, Palais de Papes, Avignon, France, September 12-15, (2005).

[7] K. A. Mathews, R. L. Miller, and C. R. Brennan, "Split-Cell, Linear Characteristic Transport Method for Unstructured Tetrahedral Meshes," *Nuclear Science and Engineering*, **136**, pp. 178-201 (2000).

[8] W. A. Rhoades and D. B. Simpson, *The TORT Three-Dimensional Discrete Ordinates Neutron/Photon Transport Code*, ORNL/TM-13221, Oak Ridge National Laboratory (1997).

2009 International Conference on Mathematics, Computational
Methods & Reactor Physics (M&C 2009), Saratoga Springs, NY, 2009

15/15